

Online Research @ Cardiff

This is an Open Access document downloaded from ORCA, Cardiff University's institutional repository: <https://orca.cardiff.ac.uk/id/eprint/124813/>

This is the author's version of a work that was submitted to / accepted for publication.

Citation for final published version:

Oniosun, Sunday, Harbottle, Michael ORCID: <https://orcid.org/0000-0002-6443-5340>, Tripathy, Snehasis ORCID: <https://orcid.org/0000-0003-1632-7668> and Cleall, Peter ORCID: <https://orcid.org/0000-0002-4005-5319> 2019. Plant growth, root distribution and non-aqueous phase liquid phytoremediation at the pore-scale. Journal of Environmental Management 249 , 109378. 10.1016/j.jenvman.2019.109378 file

Publishers page: <http://dx.doi.org/10.1016/j.jenvman.2019.109378>
<<http://dx.doi.org/10.1016/j.jenvman.2019.109378>>

Please note:

Changes made as a result of publishing processes such as copy-editing, formatting and page numbers may not be reflected in this version. For the definitive version of this publication, please refer to the published source. You are advised to consult the publisher's version if you wish to cite this paper.

This version is being made available in accordance with publisher policies.

See

<http://orca.cf.ac.uk/policies.html> for usage policies. Copyright and moral rights for publications made available in ORCA are retained by the copyright holders.



1 Plant growth, root distribution and non-aqueous phase
2 liquid phytoremediation at the pore-scale

3 *Sunday Oniosun^a, Michael Harbottle^{b*}, Snehasis Tripathy^c, and Peter Cleall^d*

4 ^a Cardiff School of Engineering, Cardiff University, Queen's Buildings, The Parade, Cardiff,
5 Wales, United Kingdom. CF24 3AA.

6 ^b Cardiff School of Engineering, *corresponding author – email: HarbottleM@cardiff.ac.uk; tel:
7 +44 2920 875759.

8 ^c Cardiff School of Engineering, email: TripathyS@cardiff.ac.uk.

9 ^d Cardiff School of Engineering, email: Cleall@cardiff.ac.uk.

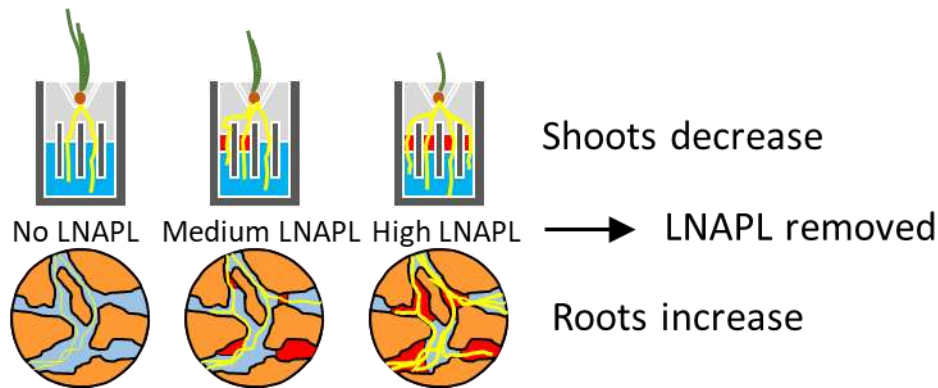
10

11

Abstract

The success of phytoremediation is dependent on the exposure of plants to contaminants, which is controlled by root distribution, physicochemical characteristics, and contaminant behaviour in the soil environment. Whilst phytoremediation has been successful in remediating hydrocarbons and other organic contaminants, there is little understanding of the impact of non-aqueous phase liquids (NAPLs) on plant behavior, root architecture and the resulting impact of this on phytoremediation. Light NAPLs (LNAPLs) may be present in pore spaces in the capillary zone as a continuous or semi-continuous phase, or as unconnected ganglia which act as individual contaminant sources. Experimental work with ryegrass (*Lolium perenne*) grown under hydroponic conditions in idealised pore scale models is presented, exploring how plant growth, root distribution and development, and oil removal are affected through direct physical contact with a model LNAPL (mineral oil). In the presence of low levels of LNAPL, a significant decrease in root length was observed, whilst at higher LNAPL levels root lengths increased due to root diversion and spreading, with evidence of root redistribution in the case of LNAPL contamination across multiple adjacent pores. Changes to root morphology were also observed in the presence of LNAPL with plant roots coarse and crooked compared to long, fine and smooth roots in uncontaminated columns. Root and shoot biomass also appear to be impacted by the LNAPL although the effects are complex, affected by both root diversion and thickening. Substantial levels of LNAPL removal were observed, with roots close to LNAPL sources able to remove dissolved-phase contamination, and root growth through LNAPL sources suggest that direct uptake/degradation is possible.

Keywords: non-aqueous phase liquids, phytoremediation, *Lolium perenne*, root architecture



Abstract art:

1. Introduction

Phytoremediation is the treatment of environmental contamination through the use of plants to clean up or contain contaminants in soil *in situ*. It has been used in the treatment of numerous organic contaminants, with a number of different mechanisms postulated, including plant-associated direct uptake or metabolism (Gobelius et al., 2017; Wang et al., 2004), volatilization (Limmer and Burken, 2016) or rhizosphere interactions (dos Santos and Maranhão, 2018). In all cases, however, the interaction between contamination and the plant root system is central to the success of the treatment. Many organic contaminant species are relatively insoluble in water, and so are commonly referred to as non-aqueous phase liquids (NAPLs), a separate liquid phase to groundwater which is relatively immobile, difficult to remediate and a persistent and recalcitrant source of dissolved phase contamination which pose serious management challenges (Tomlinson et al., 2017). Light non-aqueous phase liquids (LNAPLs), such as fuel oils, are less dense than water and so are commonly present in the capillary zone and around the phreatic surface. They are therefore likely to interact with plant root systems and so could be considered targets for phytoremediation but to date there has been little consideration of the impact of NAPLs on plant roots, or *vice versa*. Their physical distribution may be complex, with scenarios ranging from

larger zones of continuous NAPL contamination to small unconnected individual ganglia isolated in single pore spaces with the latter becoming more common as the contaminant source ages.

Interaction between the plant rhizosphere and contaminants is essential for remediation – the potential for plants to clean up dissolved phase contamination is well established as these are mobile and easily taken up by roots or microorganisms. The ability of various species to phytoremediate oil contamination at levels where NAPLs would be expected has also been demonstrated (Hunt et al., 2018; Lu et al., 2010). However, the interaction of LNAPLs with roots, and their effect on root development and morphology, plant growth and subsequent contaminant behavior is yet to be established. For example, NAPLs may hinder root development and instigate root avoidance of NAPL-contaminated pores or zones, but roots in close proximity to NAPLs may be able to reduce dissolved-phase contamination through mechanisms including uptake and rhizodegradation such that non-equilibrium conditions arise, causing relatively rapid dissolution of the NAPL. It may even be the case that roots and the rhizosphere interact with the NAPL to bring about its removal or breakdown directly. The impact of likely NAPL-forming contaminants on roots has been considered previously (Vázquez-Cuevas et al., 2018), but the impact of the physical form of the chemical, and therefore the presence or absence of NAPL, was not addressed. Roots of plants in soil mixed with heavy oil were found to be coarse and injured (Franco et al., 2011; Naidoo, 2016) with increased root diameter commonly observed. Effects of oils or similar contaminants that are known or likely to impact upon root morphology include decreased hydraulic conductivity due to heavy oil blocking flow paths (Khamehchiyan et al., 2007), higher soil temperature due to darker soil causing increased absorption of heat (Balks et al., 2002), increased mechanical impedance (Merkl et al., 2005), water deficiency causing drought stress (Merkl et al., 2005), or increased competition for nutrients such as phosphorus with microorganisms

biodegrading the oil (Merkl et al., 2005). However, the actual mechanisms of the multiphase interactions of plant, soil minerals, soil pore liquid and soil pore gas with NAPL contaminants in the rhizosphere remain ill-defined.

The principal aim of this study is to explore how root growth and distribution is affected through physical proximity to an LNAPL in the pore space. Root distribution patterns of ryegrass plants were observed within artificial pores both with and without LNAPL contamination under hydroponic conditions in 3D-printed pore-scale rhizoboxes. In addition, the spatial distribution of NAPL contamination loss is related to the spatial distribution of roots. Quantitative and semi-quantitative measurements for root growth, root morphology in a particular column, NAPL loss, shoot height and root length were measured over time, and root and shoot biomass determined at the end of the experimental trial. Preliminary results from a small part of this work have been reported in Oniosun et al. (2018).

2. Materials and methods

Mineral oil (Fisher Bio-Reagents) was chosen as the model LNAPL as it has low volatility and water solubility meaning mechanisms of contaminant loss other than through bio/phytoremediation are minimised. Mineral oil is a non-aromatic, slightly toxic hydrocarbon with a density of 0.83 Mg/m^3 and viscosity of $33.5 \times 10^{-3} \text{ Pa.s}$. The colorant Oil Red O (Sigma-Aldrich) was added to the mineral oil at a concentration of 50 mg/L to enhance oil visibility allowing the movement and location of the LNAPL to be detected (Page et al., 2007). Perennial ryegrass (*Lolium perenne*, obtained from Boston Seeds, UK) was chosen as the model phytoremediation agent because of its proven capability to remediate organic contaminants (Rezek

et al., 2008). The plant growth solution, used as the aqueous phase, was quarter strength Hoagland's solution (2.5 g/L Hoagland's No.2 Basal Salt Mixture (Sigma-Aldrich, UK) in deionized water).

2.1 Apparatus

Plants were grown under hydroponic conditions in pore-scale 3D-printed rhizoboxes (Figure 1). These were printed from polylactic acid (PLA) on an Ultimaker 3D printer. Each box had PLA back, side walls, base and three partitions (15 mm by 1 mm by 2mm) creating four equally spaced columns (1.75 mm wide and 2.0 mm thick) above a 2.5 mm deep open void. Above these, a V-shaped seed housing was created to ensure consistent location of a single seed for germination and plant growth. To allow visual observation of plant development, acetate sheets (26 x 15 x 1 mm) were bonded to the rhizobox front with cyanoacrylate glue and sealed with LS-X jointing compound and external leak sealer ensuring water and oil tightness. Each sheet was placed to leave a 2mm gap at the base of the box, allowing nutrient solution movement to and from an external reservoir.

Rhizobox materials were tested for their potential to impact upon experimental observations through oil absorption. Polylactic acid filament and acetate film samples were found to absorb 1.14 and 0.02% mineral oil by mass on average, although this is a conservative measure and likely to be lower.

2.2 Experimental design

Ten contamination scenarios were considered as shown in Table 1 and comprise all possible combinations of oil contamination in the four columns (note that combinations that are 'reflections' of others, e.g. oil in columns 2 and 4 rather than 1 and 3, are considered to be identical

and were not tested). Scenario 10 is a no-oil control to which other scenarios can be compared. The ten scenarios were considered to give a practical representation of the state of LNAPL in pore spaces in the capillary zone, and could be considered as a continuous or semi-continuous phase, or as unconnected ganglia. The gap between the planted seed and the contaminant and/or fluid allows germination and initial establishment of ryegrass in all scenarios, as this can be affected by phytotoxicity of organic contaminants (Adam and Duncan, 2002). Moreover, it was designed for the root to grow freely and not be forced into any of the columns, since it has been shown that deeper contaminated layers allow for better initial root establishment (Kechavarzi et al., 2007). Five replicates were tested for each of the ten scenarios.

2.3 Sample preparation and rhizobox arrangements

The fifty rhizoboxes were affixed to the base of a 660 (W) x 650 (D) x 210 mm (H) plastic container, which acted as a reservoir of nutrient solution. The reservoir container was filled with 3500 ml of the nutrient solution (quarter-strength Hoagland's No. 2 Basal Salt Mixture, Sigma Aldrich, UK), maintaining the height of nutrient solution in the rhizoboxes at 18 mm above the lowest point of the base with no oil present. When oil was present, the upper surface of the oil layer was at a height of 20 mm above this point. A Mariotte bottle supplied nutrient solution to the reservoir when necessary to maintain a constant fluid level within the rhizoboxes and surrounding reservoir. The reservoir fluid was pumped through an ultraviolet water steriliser (Vecton 120 Nano) at around 5 ml per minute (one volume per 11.7 hours) to control microbial growth. The pH was checked daily to ensure that it was maintained between the range of 5.3 – 6.5 to maximise nutrient solubility. Airborne microbial contamination and water loss to evaporation were minimized by a purpose-made plastic cloche with vents to allow air circulation. The container and cloche were contained within a transparent PVC tunnel greenhouse.

Ten microliters of coloured mineral oil was deposited on the nutrient solution surface in all the rhizobox columns designated as being contaminated by oil (Table 1) with a Hamilton 701RN syringe. This gave an oil layer within the column of depth 2.9 mm. One seedling of perennial ryegrass was placed into the seed housing, along with a small amount of cotton wool moistened with quarter-strength Hoagland's solution.

The reservoir container was exposed to light provided by four 58 W cool white daylight spectrum fluorescent tubes, placed 1500 mm above the rhizoboxes for 16 hours per day. A temperature data-logger was used to record the ambient temperature. Plant images were captured with a water resistant 12 MP wide-angle digital camera, placed on a small camera stand located 15 cm from the front of the rhizobox. A Softbox Twin-Head Continuous lighting kit, comprising 2 x continuous single lamp heads (105W, 5500K daylight balanced Compact Fluorescent Light bulbs) with integrated 50 cm x 70 cm softboxes was used as a broader light source.

2.4 Plant and Oil analysis

The experiment lasted four weeks, with day 0 defined as the time of seeding. At 7, 14, 21 and 28 days, images were taken and observations made of root and shoot growth patterns and oil levels in all rhizoboxes. Semi-quantitative measurements of root growth and distribution and oil loss were made during the experiment as fully quantitative and accurate data could not be obtained for either measurement without disturbing the specimen. The presence of roots in each column of each rhizobox was assessed as *established* (score = 1, where the longest root was observed to reach a depth of at least 14 mm below the seed housing (8 mm below the surface of the oil layer where present), *limited* (score = 0.5, where the longest root has penetrated the oil layer and/or water beneath but where the depth is less than 14 mm below the seed housing), and *none* (score = 0,

where there is no root, or the root has not yet penetrated the oil and/or water layer). Similarly, oil loss was categorized as *full* (score = 1, where there was no visible oil left), *partial* (score = 0.5, where oil was visible but clearly reduced in thickness) or *none* (score = 0, where the oil has remained at or near its initial volume, i.e. approximately 2.9mm, determined using scales attached to each rhizobox). The root and shoot biomass were determined at the end of the experimental growth trial by carefully washing the seedlings with de-ionized water and separating them into shoots and roots at the crown (growing point). The fresh root and shoot samples were dried at 75°C for 24 hours and then weighed to determine the biomass production. Total root and shoot lengths were determined by summing the total length of all roots or shoots in a replicate. The oil and root scoring data was statistically examined using non-parametric t-tests. Quantitative shoot and root data was statistically examined to determine the significance of differences between treatments, calculated using analysis of variance (Minitab v.17). Significance was evaluated at the 95% confidence level. Pairwise comparisons were made using the Tukey method, again at the 95% confidence level, in order to determine the significance of differences between means.

3. Results and discussion

Seedling germination and growth was found to be consistently good across all replicates in all scenarios. Germination occurred in all rhizoboxes.

Figure 2 shows stacked root growth and oil loss scores at day 28. Each ‘stack’ includes the scores from all five replicates, presented for each of the 4 columns in all ten scenarios. For example, if full root growth or complete oil loss (i.e. score = 1) was observed in a particular column in all five replicates, the bar will have a total index of 5. Stacked root growth bars are presented in order to

graphically show the distribution of growth across all replicates as it was not found to be sufficiently informative to present data as, for example, averages with error bars given the limited number of possible scores in the raw data. In all scenarios, it is apparent that roots were spatially located primarily in the two middle columns (columns 2 and 3) regardless of contaminant location, indicating that roots tend to grow vertically downwards with little lateral spread initially, and that this is largely unaffected by the presence of individual oil ‘ganglia’ in these columns. The roots appear to coexist with the contaminants within oil-contaminated columns rather than avoiding them. An effect of mineral oil on root growth is apparent in scenarios 7, 8 and 9 where three or all four columns had oil, with root growth being considerably more evenly distributed across the columns. The standard deviation of the root growth score across each rhizobox was determined as a measure of root growth distribution across the different columns. For scenarios 1-6 and 10, this value was typically between 0.4 and 0.6 ($n = 35$, with one outlier at 0.3), which may be expected given the preponderance of growth in columns 2 and 3. For scenarios 7-9, this measure of root growth distribution was typically between 0 and 0.3 ($n = 15$, with two outliers at 0.48), demonstrating much more even growth. However, it is not simply the presence of oil in columns 2 and 3 which subsequently caused the plant to seek out new routes to the nutrient medium, as scenario 4 had oil only in these columns and no diversion or spreading of roots was observed. Instead, it is hypothesized that the larger oil presence in scenarios 7 to 9 led to higher levels of *dissolved* mineral oil, at least transiently, and that it was this that limited growth in columns 2 and 3 and therefore caused root spreading. There is some evidence for this in that the root growth in columns 2 and 3 of scenario 4 was found to be consistently higher than that in scenarios 7 to 9. In oil contaminated columns, the presence of a root led to substantial oil loss (Figure 2) whereas in plant-free experiments little or no oil loss was observed (results not presented). Even where little

or no root growth was observed in an oil-contaminated column, the oil still disappeared, albeit more slowly than when a plant root was present. This suggests that oil removal occurred through the actions of roots in adjacent columns, due to phytoremediation of the dissolved fraction of oil leading to increased rates of oil dissolution. Greater oil loss was generally observed in scenarios with less contamination overall, similar to the outcomes in other studies (Terzaghi et al., 2018; Zengel et al., 2016). This may also be related to the possible phytoremediation of dissolved phase oil, as if all roots contribute to remediation of all columns, a smaller amount of oil will generally be remediated more quickly (Gouda et al., 2016).

The presence of oil in an individual column had only a small effect on the root growth within that column (Figure 3). The average of the observed root growth indices for a given column with or without oil for all five replicates and all ten scenarios are presented because the total number of columns with and without oil are different and so a stacked plot (as in Figure 2) would not suffice (e.g. there are more column 3s and 4s without oil than with it). Although the effect of oil is small, in columns 2 and 3 there is apparently a small negative effect of the presence of oil on root growth in individual columns (statistically significant in column 2 - $p = 0.007$ for day 28 respectively). It may be that the thickness of the oil layer was insufficient to affect the root growth significantly, and that greater amounts of oil would have a larger effect. In addition, ryegrass has some tolerance to oil contamination (McIntosh et al., 2017; Zhu et al., 2018).

Although the visual scoring of root length showed relatively little impact of increasing oil levels on total root length across all columns in a particular scenario, it was observed that, in the oil-contaminated columns, plant roots were coarse and crooked, while those in uncontaminated columns were long, fine and smooth. Slightly increased root growth with increasing oil levels was observed in scenario 7 and 9 (oil in three or four columns), compared to the uncontaminated

scenario 10, and this may be a response of the plants to environmental stress, increasing the spread of roots in an effort to find an uncontaminated route to nutrient supply. Root injuries and changes in root architecture (length, thickness and branching) are commonly observed as a result of abiotic stresses such as drought, salinity or metal contamination (Álvarez and Sánchez-Blanco, 2013; Franco et al., 2011) although the actual impact is highly species dependent.

Figure 4 combines the root growth and oil loss data for columns where oil was present, for each time point, and shows that root growth appears to be correlated to oil loss at days 14 and 21 – increased root growth in columns 2 and 3 is matched by increasing levels of oil loss. It should be noted that there is overlap of data points on this figure, because of the limited number of possible values for both parameters. However, as time progressed there was some root growth and concomitant oil loss in columns 1 and 4, though the oil loss was large for relatively small root growth and in certain cases, oil was lost without any root growth in a column. This suggests that enhanced removal of the low levels of dissolved phase mineral oil by established roots in columns 2 and 3 disrupts the equilibrium causing further mineral oil in all columns to dissolve, which in turn is removed by the action of the roots and possibly attendant microorganisms.

Figure 5a shows the day 28 total root and shoot length for each scenario, averaged across all replicates, whilst Figure 5b shows root and shoot biomass in a similar manner. There are trends in the average values in each scenario which may be of relevance but these must be viewed with caution given the high variability in the data. Analysis of variance indicated that there were no statistically significant differences of root/shoot mass or shoot length between any scenarios. Scenario 10, without any contamination, had the highest average total shoot length and mass as might be expected, whilst the average values from scenarios 4, 7 and 9 were substantially lower. The largest average root masses (Figure 5b) were also found in these scenarios, which are the ones

with oil present in both central columns, so given the prevalence of root growth in these columns it is perhaps not surprising that this has impacted upon plant shoot development. With roots, the average total length in scenarios 7, 8 and 9 were not significantly different to the largest values in scenario 10 whilst others were significantly lower ($p=0.05$ or above), which is indicative of the greater distribution of root growth across all columns in these scenarios as noted earlier.

Although not statistically significant, the increase in average root biomass, compared to a corresponding decrease in average shoot biomass, in response to increasing mineral oil suggests the plant put more energy into root growth than shoot growth due to stress induced by oil contamination. Oil can not only reduce the amount of water and oxygen available for plant growth (Kaur et al., 2017) but also can interfere with plant-water relations by direct physical contact (coating of root tissues) thus negatively affecting shoot growth (Razmjoo and Adavi, 2012). Such phenomena affect the local biogeochemistry, for example changing nutrient dynamics (Xu and Johnson, 1997) which in turn cause changes in root morphology similar to those observed here (Franco et al., 2011; Hermans et al., 2006).

It is noted that soil texture and consequent variations in pore structure are likely to affect the interaction between oil and root/rhizosphere in a real application. Such impacts have been explored in more detail in Oniosun et al. (2018) and Oniosun (2019). They report an influence of the presence of a fine-grained particle fraction on the location of oil within the pore space and discuss potential changes in contaminant bioavailability and transport in the larger pores impacting how toxic compounds can migrate in the soil and inhibit water and nutrients from reaching the rhizosphere thereby reducing the supply of oxygen, moisture, and nutrients which may lead to root damage or death. Such variations in soil texture might give plant roots greater accessibility to

larger pores in coarser soils meaning increased accessibility to nutrients and moisture in the rhizosphere (Mitton et al., 2014), therefore a lesser adverse effect on plant root growth.

It has been previously found that mineral oil negatively affects plant root architecture (thickness, length and branching) as a result of injuries caused by contamination (Vervaeke et al., 2003). Studies have observed increased root biomass in mineral oil-treated soil, attributed to a typical plant response to the reduced rhizosphere mycorrhiza and nutrient deficiency due to oil contamination (Heinonsalo et al., 2000). Poorter and Nagel (2000) concluded that plants respond to a decrease in below ground nutrients with increased allocation of biomass to roots and a reduction in above-ground resources (e.g. sunlight) with increased allocation of biomass to shoots. This effect resulted in coarser roots, expressed in increased average root diameter with a reduction in specific root length, but a larger surface area. Greater phytodegradation of organic contaminants has previously been related to higher specific root surface area (Ahmad et al., 2012; Merkl et al., 2005).

4. Conclusions

In contaminated soils light NAPLs may be present in pore spaces in the capillary zone as a continuous or semi-continuous phase, or as unconnected ganglia which act as individual contaminant sources, providing a long-term supply of dissolved phase contamination. A laboratory experiment to provide evidence of the impact of LNAPL distribution in the pore space on root growth distribution was performed. Oil levels and root growth was monitored on a regular basis, and the resulting contaminant loss, root morphology, root, and shoot biomass analysed. Good levels of consistency in germination and growth were found across all experiments.

It is apparent from comparisons of oil loss in contaminated columns with the presence of a root to that in plant-free experiments that phytoremediation of dissolved phase contamination accelerates the dissolution of LNAPLs into adjacent groundwater and thus can indirectly destroy these persistent contaminant sources considerably more rapidly than by natural attenuation alone. Any contribution from direct interaction between root and NAPL has not been conclusively demonstrated here, but direct uptake of hydrocarbons is known to be possible (Hunt et al., 2018) although likely to be slower than dissolved phase effects. In general, greater oil loss was observed in scenarios with lower levels of overall contamination. Indeed, the presence of NAPL does not prevent growth of a root within a pore, with a preference for vertical downwards root growth dominating, allowing co-existence and therefore more rapid NAPL removal (either directly, indirectly or both) than would otherwise be the case. The impact of NAPL on root architecture is clear, with greater distribution of root growth with more extensive NAPL coverage (thought to be caused by increased access to dissolved phase oil) and changes to individual root morphology. Impact on the plant as a whole was detrimental, with considerably reduced above ground biomass as well as the changes to the roots. The observed increase in root biomass and a corresponding decrease in shoot biomass in the presence of increasing levels of LNAPL indicates plants diverting energy into root growth from shoot growth due to stress induced by oil contamination. This study gives valuable direct evidence on how plant growth, root distribution and development, and oil removal are affected through direct physical contact with LNAPL

Acknowledgements

320 The first author gratefully acknowledges moral support and encouragement from Powell Dobson
321 Architects Ltd, Cardiff.

322

323 **Funding**

324 The first author was supported by Blowsome Estate Nig. Ltd (no grant number).

325

326 **References**

- 327 Adam, G., Duncan, H., 2002. Influence of diesel fuel on seed germination. *Environ. Pollut.* 120,
328 363-370, [https://doi.org/10.1016/S0269-7491\(02\)00119-7](https://doi.org/10.1016/S0269-7491(02)00119-7).
- 329 Ahmad, F., Iqbal, S., Anwar, S., Afzal, M., Islam, E., Mustafa, T., Khan, Q.M., 2012. Enhanced
330 remediation of chlorpyrifos from soil using ryegrass (*Lolium multiflorum*) and chlorpyrifos-
331 degrading bacterium *Bacillus pumilus* C2A1. *J. Hazard. Mater.* 237, 110-115,
332 <https://doi.org/10.1016/j.jhazmat.2012.08.006>.
- 333 Álvarez, S., Sánchez-Blanco, M.J., 2013. Changes in growth rate, root morphology and water
334 use efficiency of potted *Callistemon citrinus* plants in response to different levels of water
335 deficit. *Scientia horticultrae* 156, 54-62, <https://doi.org/10.1016/j.scienta.2013.03.024>.
- 336 Balks, M.R., Paetzold, R.F., Kimble, J.M., Aislabie, J., Campbell, I.B., 2002. Effects of
337 hydrocarbon spills on the temperature and moisture regimes of Cryosols in the Ross Sea region.
338 *Antarct. Sci.* 14, 319-326, <https://doi.org/10.1017/S0954102002000135>.
- 339 dos Santos, J.J., Maranhão, L.T., 2018. Rhizospheric microorganisms as a solution for the
340 recovery of soils contaminated by petroleum: A review. *J. Environ. Manage.* 210, 104-113,
341 <https://doi.org/10.1016/j.jenvman.2018.01.015>.
- 342 Franco, J., Bañón, S., Vicente, M., Miralles, J., Martínez-Sánchez, J., 2011. Root development in
343 horticultural plants grown under abiotic stress conditions—a review. *J Hortic Sci Biotechnol* 86,
344 543-556, <https://doi.org/10.1080/14620316.2011.11512802>.
- 345 Gobelius, L., Lewis, J., Ahrens, L., 2017. Plant uptake of per- and polyfluoroalkyl substances at a
346 contaminated fire training facility to evaluate the phytoremediation potential of various plant
347 species. *Environ. Sci. Technol.* 51, 12602-12610, <https://doi.org/10.1021/acs.est.7b02926>.
- 348 Gouda, A.H., El-Gendy, A.S., El-Razek, T.M.A., El-Kassas, H.I., 2016. Evaluation of
349 phytoremediation and bioremediation for sandy soil contaminated with petroleum hydrocarbons.
350 *International Journal of Environmental Science and Development* 7, 490,
351 <http://www.ijesd.org/vol7/826-X0052.pdf>.
- 352 Heinonsalo, J., Jørgensen, K.S., Haahtela, K., Sen, R., 2000. Effects of *Pinus sylvestris* root
353 growth and mycorrhizosphere development on bacterial carbon source utilization and

hydrocarbon oxidation in forest and petroleum-contaminated soils. *Can. J. Microbiol.* 46, 451-464, <https://doi.org/10.1139/w00-011>.

Hermans, C., Hammond, J.P., White, P.J., Verbruggen, N., 2006. How do plants respond to nutrient shortage by biomass allocation? *Trends Plant Sci.* 11, 610-617, <https://doi.org/10.1016/j.tplants.2006.10.007>.

Hunt, L.J., Duca, D., Dan, T., Knopper, L.D., 2018. Petroleum hydrocarbon (PHC) uptake in plants: A literature review. *Environ. Pollut.*, <https://doi.org/10.1016/j.envpol.2018.11.012>.

Kaur, N., Erickson, T.E., Ball, A.S., Ryan, M.H., 2017. A review of germination and early growth as a proxy for plant fitness under petrogenic contamination—knowledge gaps and recommendations. *Sci. Total Environ.* 603, 728-744, <https://doi.org/10.1016/j.scitotenv.2017.02.179>.

Kechavarzi, C., Pettersson, K., Leeds-Harrison, P., Ritchie, L., Ledin, S., 2007. Root establishment of perennial ryegrass (*L. perenne*) in diesel contaminated subsurface soil layers. *Environ. Pollut.* 145, 68-74, <https://doi.org/10.1016/j.envpol.2006.03.039>.

Khamehchiyan, M., Charkhabi, A.H., Tajik, M., 2007. Effects of crude oil contamination on geotechnical properties of clayey and sandy soils. *Eng Geol* 89, 220-229, <https://doi.org/10.1016/j.enggeo.2006.10.009>.

Limmer, M., Burken, J., 2016. Phytovolatilization of Organic Contaminants. *Environ. Sci. Technol.* 50, 6632-6643, <https://doi.org/10.1021/acs.est.5b04113>.

Lu, M., Zhang, Z., Sun, S., Wei, X., Wang, Q., Su, Y., 2010. The use of goosegrass (*Eleusine indica*) to remediate soil contaminated with petroleum. *Water, Air, Soil Pollut.* 209, 181-189, <https://doi.org/10.1007/s11270-009-0190-x>.

McIntosh, P., Schulthess, C.P., Kuzovkina, Y.A., Guillard, K., 2017. Bioremediation and phytoremediation of total petroleum hydrocarbons (TPH) under various conditions. *Int. J. Phytoremediation* 19, 755-764, <https://doi.org/10.1080/15226514.2017.1284753>.

Merkel, N., Schultze-Kraft, R., Infante, C., 2005. Phytoremediation in the tropics - influence of heavy crude oil on root morphological characteristics of graminoids. *Environ. Pollut.* 138, 86-91, <https://doi.org/10.1016/j.envpol.2005.02.023>.

Mitton, F.M., Miglioranza, K.S., Gonzalez, M., Shimabukuro, V.M., Monserrat, J.M., 2014. Assessment of tolerance and efficiency of crop species in the phytoremediation of DDT polluted soils. *Ecol. Eng.* 71, 501-508, <https://doi.org/10.1016/j.ecoleng.2014.07.069>.

Naidoo, G., 2016. Mangrove propagule size and oil contamination effects: Does size matter? *Mar. Pollut. Bull.* 110, 362-370, <https://doi.org/10.1016/j.marpolbul.2016.06.040>.

Oniosun, S., Harbottle, M., Tripathy, S., Cleall, P., 2018. Phytoremediation of Light Non-Aqueous Phase Liquids, *Proceedings of the 8th International Congress on Environmental Geotechnics*; Zhan, L., Chen, Y., Bouazza, A., Eds., Springer: Singapore, pp. 788-795, https://doi.org/10.1007/978-981-13-2221-1_89.

Oniosun, S.A., 2019. Phytoremediation of LNAPLs and Residual Oils in the Vadose Zone and Capillary Fringe. School of Engineering, Cardiff University United Kingdom, <https://ethos.bl.uk/OrderDetails.do?uin=uk.bl.ethos.775010>.

Page, J.W.E., Soga, K., Illangasekare, T., 2007. The significance of heterogeneity on mass flux from DNAPL source zones: An experimental investigation. *J. Contam. Hydrol.* 94, 215-234, <https://doi.org/10.1016/j.jconhyd.2007.06.004>.

Poorter, H., Nagel, O., 2000. The role of biomass allocation in the growth response of plants to different levels of light, CO₂, nutrients and water: a quantitative review. *Funct. Plant Biol.* 27, 1191-1191, https://doi.org/10.1071/PP99173_CO.

Razmjoo, K., Adavi, Z., 2012. Assessment of bermudagrass cultivars for phytoremediation of petroleum contaminated soils. *Int. J. Phytoremediation* 14, 14-23, <https://doi.org/10.1080/15226514.2011.560212>.

Rezek, J., Wiesche, C.I.D., Mackova, M., Zadrzil, F., Macek, T., 2008. The effect of ryegrass (*Lolium perenne*) on decrease of PAH content in long term contaminated soil. *Chemosphere* 70, 1603-1608, <https://doi.org/10.1016/j.chemosphere.2007.08.003>.

Terzaghi, E., Zanardini, E., Morosini, C., Raspa, G., Borin, S., Mapelli, F., Vergani, L., Di Guardo, A., 2018. Rhizoremediation half-lives of PCBs: Role of congener composition, organic carbon forms, bioavailability, microbial activity, plant species and soil conditions, on the prediction of fate and persistence in soil. *Sci. Total Environ.* 612, 544-560, <https://doi.org/10.1016/j.scitotenv.2017.08.189>.

Tomlinson, D.W., Rivett, M.O., Wealthall, G.P., Sweeney, R.E., 2017. Understanding complex LNAPL sites: Illustrated handbook of LNAPL transport and fate in the subsurface. *J. Environ. Manage.* 204, 748-756, <https://doi.org/10.1016/j.jenvman.2017.08.015>.

Vázquez-Cuevas, G.M., Stevens, C.J., Semple, K.T., 2018. Enhancement of 14 C-phenanthrene mineralisation in the presence of plant-root biomass in PAH-NAPL amended soil. *Int. Biodeterior. Biodegrad.* 126, 78-85, <https://doi.org/10.1016/j.ibiod.2017.09.021>.

Vervaeke, P., Luyssaert, S., Mertens, J., Meers, E., Tack, F.M.G., Lust, N., 2003. Phytoremediation prospects of willow stands on contaminated sediment: a field trial. *Environ. Pollut.* 126, 275-282, [https://doi.org/10.1016/S0269-7491\(03\)00189-1](https://doi.org/10.1016/S0269-7491(03)00189-1).

Wang, X., Dossett, M.P., Gordon, M.P., Strand, S.E., 2004. Fate of Carbon Tetrachloride during Phytoremediation with Poplar under Controlled Field Conditions. *Environ. Sci. Technol.* 38, 5744-5749, <https://doi.org/10.1021/es0499187>.

Xu, J., Johnson, R., 1997. Nitrogen dynamics in soils with different hydrocarbon contents planted to barley and field pea. *Can. J. Soil Sci.* 77, 453-458, <https://doi.org/10.4141/S96-046>.

Zengel, S., Montague, C.L., Pennings, S.C., Powers, S.P., Steinhoff, M., Fricano, G., Schlemme, C., Zhang, M., Oehrig, J., Nixon, Z., 2016. Impacts of the Deepwater Horizon oil spill on salt marsh periwinkles (*Littoraria irrorata*). *Environ. Sci. Technol.* 50, 643-652, <https://doi.org/10.1021/acs.est.5b04371>.

Zhu, H., Gao, Y., Li, D., 2018. Germination of grass species in soil affected by crude oil contamination. *Int. J. Phytoremediation* 20, 567-573, <https://doi.org/10.1080/15226514.2017.1405376>.

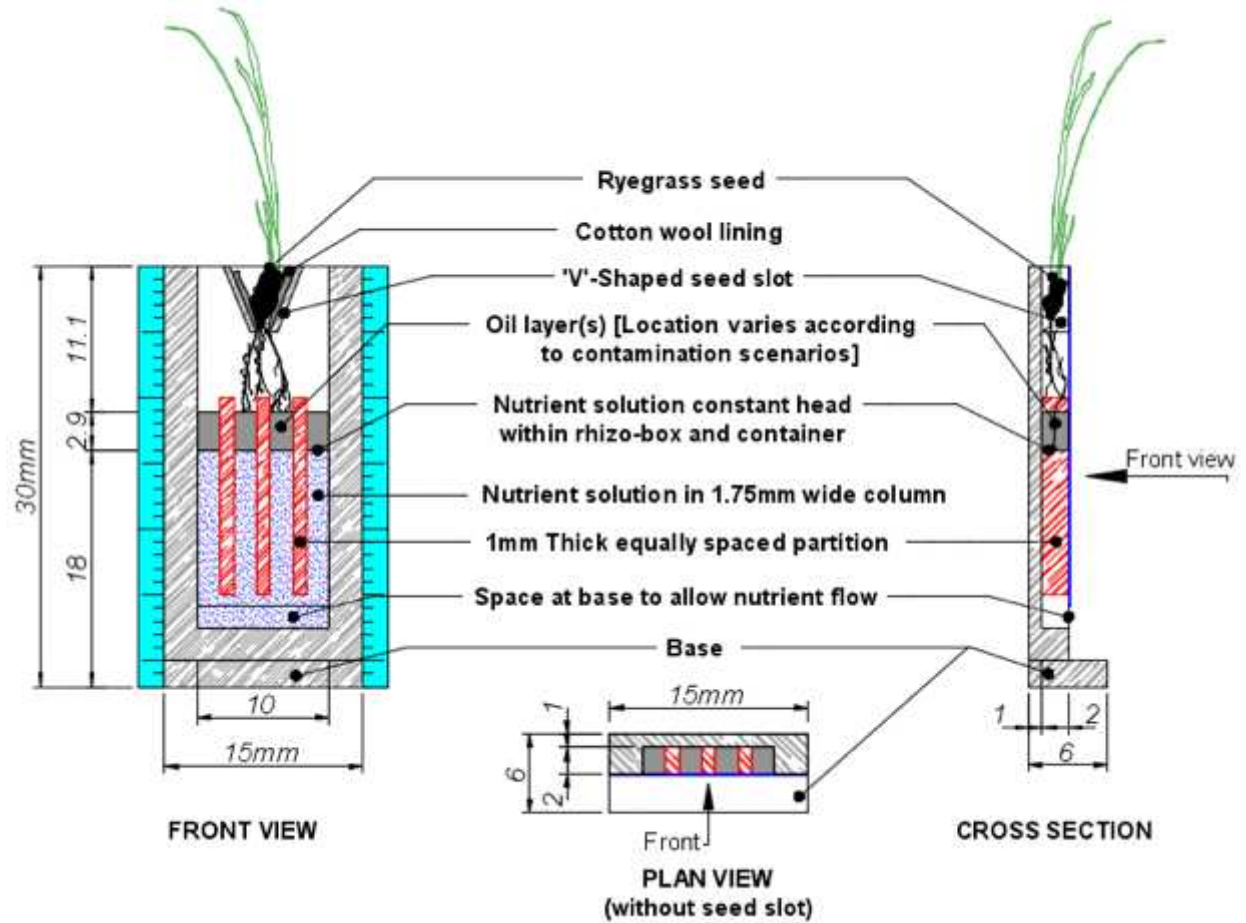


Figure 1. Schematic of pore-scale 3D-printed rhizobox

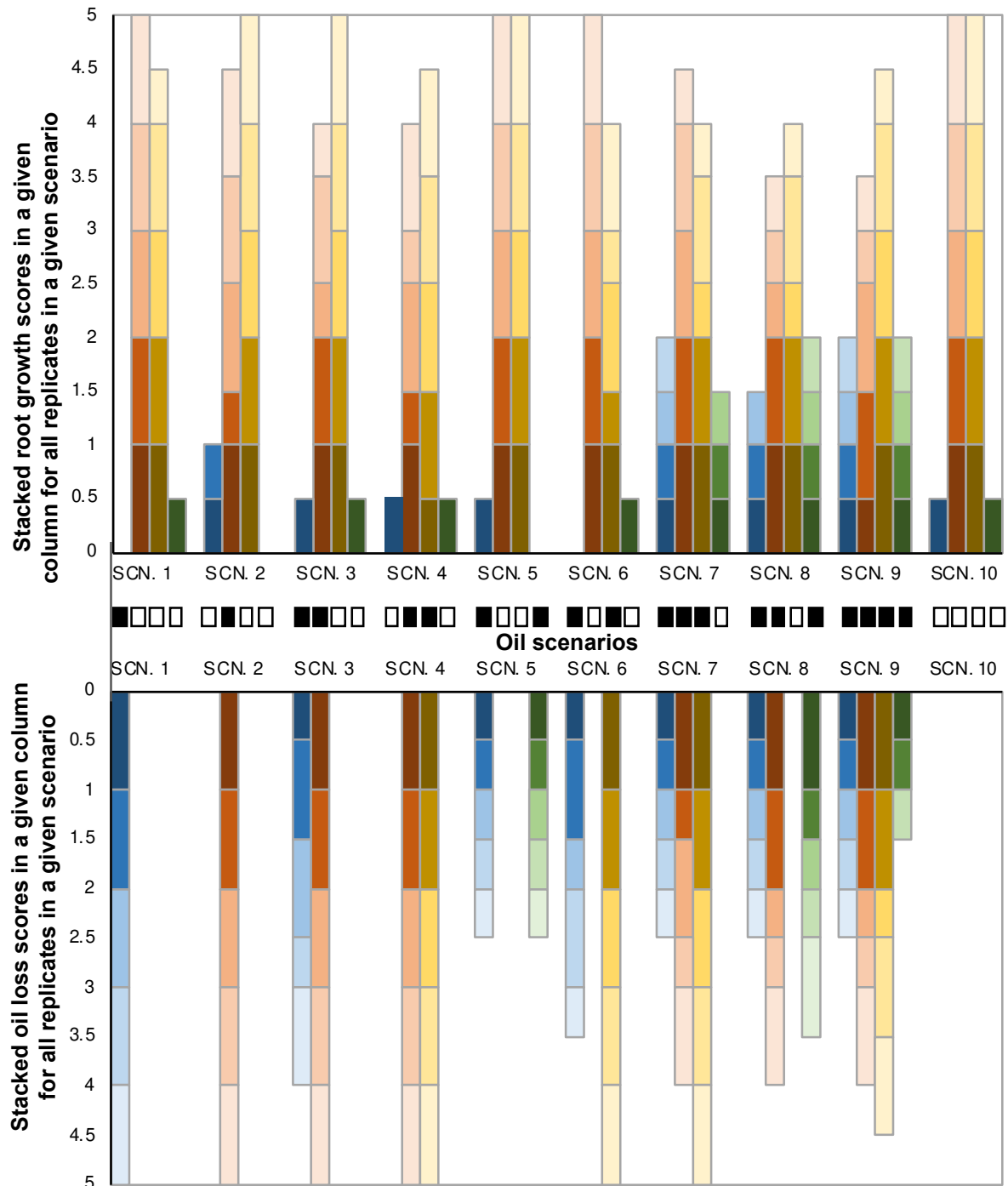


Figure 2. Root growth and oil loss in individual columns for all ten scenarios (Day 28) (blue – column 1; orange – column 2; yellow – column 3; green – column 4). For each column, root growth and oil loss are scored for all five replicates and these scores presented as a stacked bar (established root / full oil loss = 1; limited root growth / partial oil loss = 0.5; no root growth / no oil loss = 0).

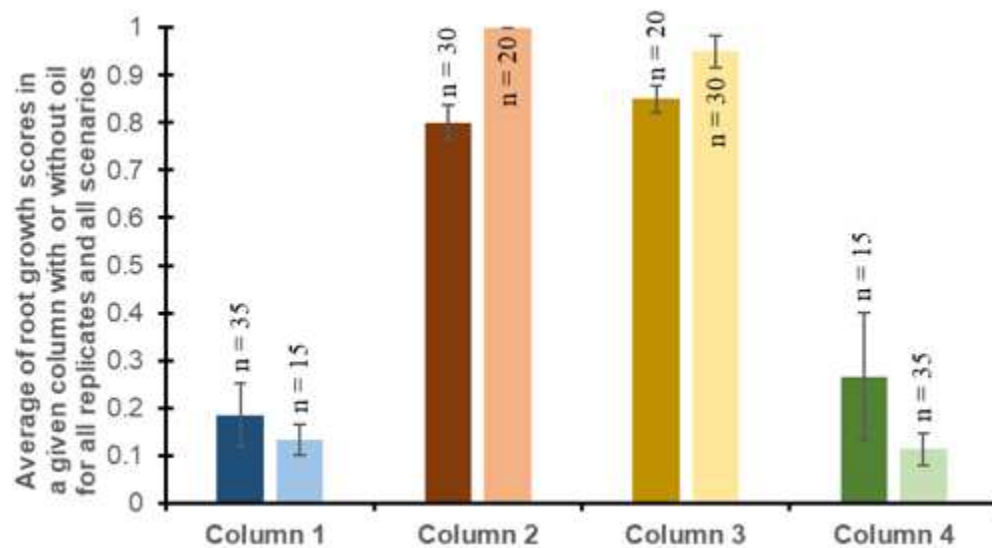


Figure 3. Effect of presence of oil on average root growth score in individual columns at day 28. For each column, root growth is scored for all replicates in all scenarios and the average presented (established root = 1; limited root growth = 0.5; no root growth = 0). The numbers with (left-hand bar, darker shade) and without oil (right-hand bar, lighter shade) (i.e. the number of readings used to calculated the averages) are presented on the figure. Error bars represent \pm one standard error of the mean.

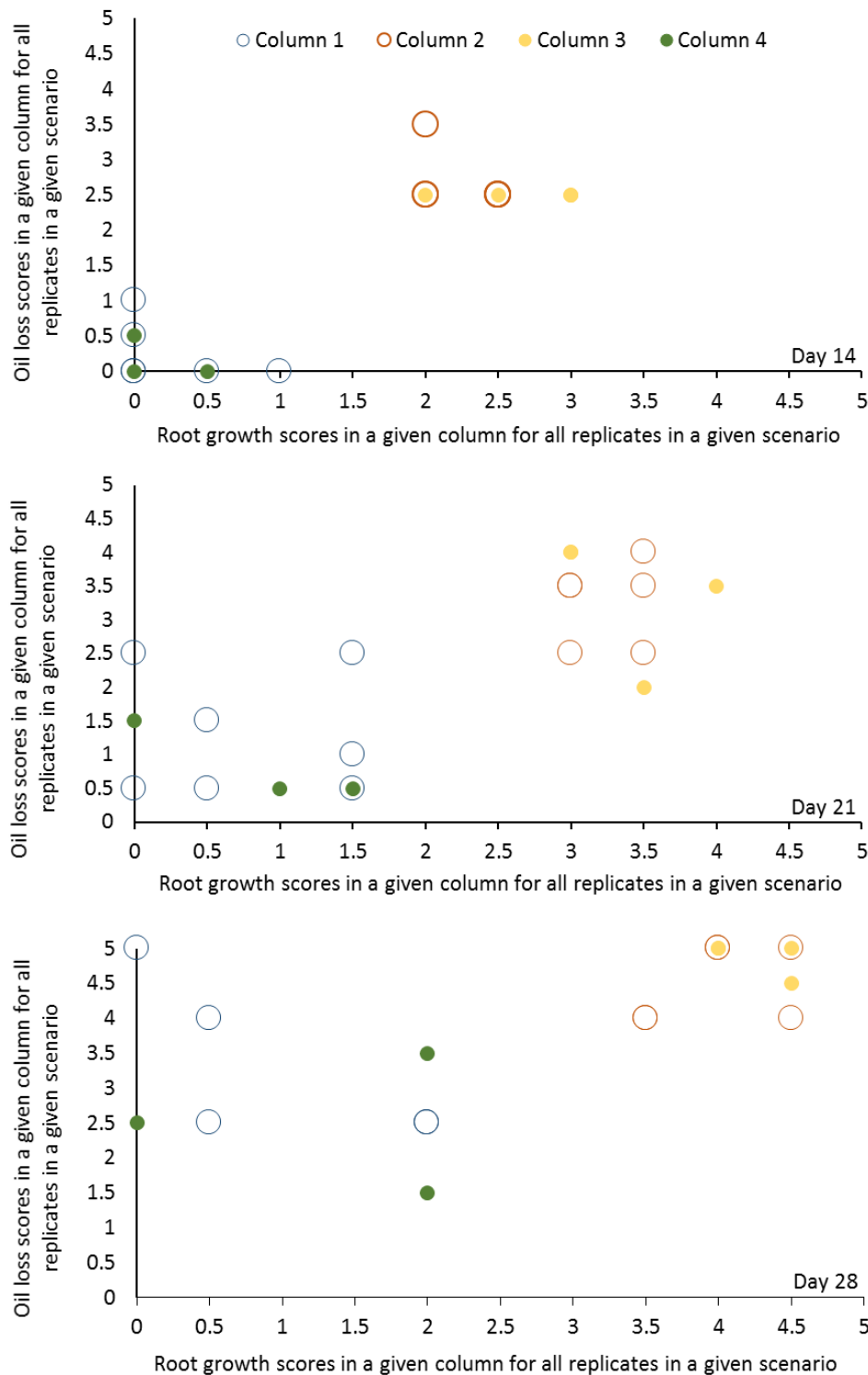


Figure 4. Relationship between root growth and oil loss in individual columns for all ten scenarios, (Days 14, 21 and 28. For each column, root growth and oil loss are scored for all five replicates and the total counts of these scores presented as a scatter plot (established root / full oil loss = 1; limited root growth / partial oil loss = 0.5; no root growth / no oil loss = 0).

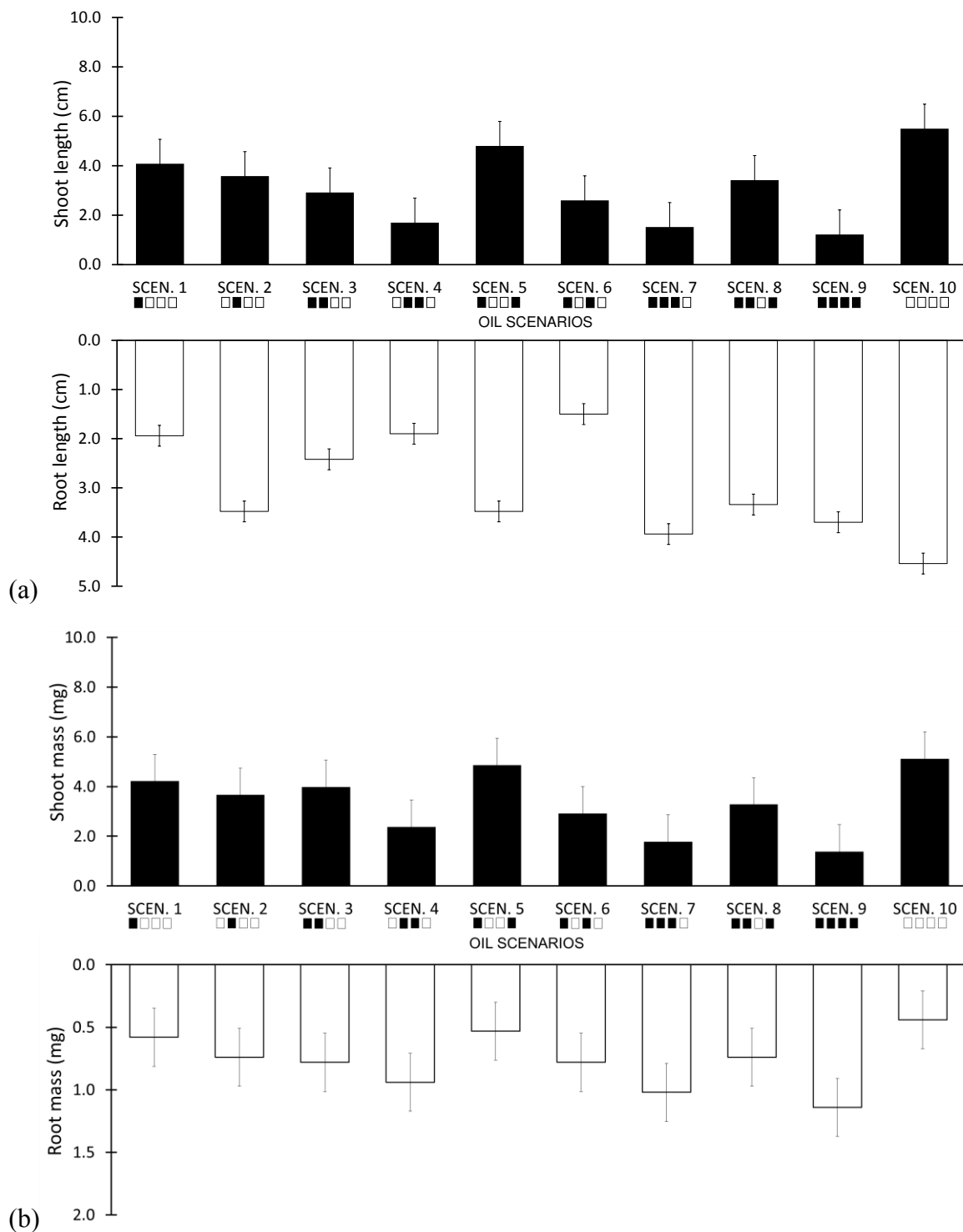


Figure 5. Effect of the presence of oil on (a) root and shoot length for all scenarios (for each scenario, root and shoot lengths were measured and summed for each replicate) and (b) root and shoot biomass (for each scenario, root and shoot mass are totalled for each replicate). Error bars represent the standard error of the mean (n=5).

461 Table 1. Mineral oil contamination scenarios inside the rhizoboxes.

| Contamination Scenario | Column 1 | Column 2 | Column 3 | Column 4 |
|------------------------|----------|----------|----------|----------|
| 1 | Oil | | | |
| 2 | | Oil | | |
| 3 | Oil | Oil | | |
| 4 | | Oil | Oil | |
| 5 | Oil | | | Oil |
| 6 | Oil | | Oil | |
| 7 | Oil | Oil | Oil | |
| 8 | Oil | Oil | | Oil |
| 9 | Oil | Oil | Oil | Oil |
| 10 | | | | |

462

463